metals

MDPI

Article

Nonisothermal Kinetic Degradation of Hybrid CNT/Alumina Epoxy Nanocomposites

Muhammad Helmi Abdul Kudus [1], Muhammad Razlan Zakaria [2,3], Mohd Firdaus Omar [2,3], Muhammad Bisyrul Hafi Othman [4,*], Hazizan Md. Akil [5], Marcin Nabiałek [6], Bartłomiej Jeż [6] and Mohd Mustafa Al Bakri Abdullah [2,3]

1 Engineering Campus, School of Mechanical Engineering, Universiti Sains Malaysia, Nibong Tebal 14300, Pulau Pinang, Malaysia; helmi.kudus@usm.my
2 Faculty of Chemical Engineering Technology, Universiti Malaysia Perlis, Arau 02600, Perlis, Malaysia; razlanzakaria@unimap.edu.my (M.R.Z.); firdausomar@unimap.edu.my (M.F.O.); mustafa_albakri@unimap.edu.my (M.M.A.B.A.)
3 Geopolymer & Green Technology, Centre of Excellent (CEGeoGTech), Universiti Malaysia Perlis, Arau 02600, Perlis, Malaysia
4 School of Chemical Sciences, Universiti Sains Malaysia, Minden 11800, Pulau Pinang, Malaysia
5 Engineering Campus, School of Materials and Minerals Resources Engineering, Universiti Sains Malaysia, Nibong Tebal 14300, Pulau Pinang, Malaysia; hazizan@usm.my
6 Department of Physics, Częstochowa University of Technology, 42-201 Częstochowa, Poland; nmarcell@wp.pl (M.N.); bartek199.91@o2.pl (B.J.)
* Correspondence: bisyrul@usm.my; Tel.: +60-4-6534032

Abstract: Due to the synergistic effect that occurs between CNTs and alumina, CNT/alumina hybrid-filled epoxy nanocomposites show significant enhancements in tensile properties, flexural properties, and thermal conductivity. This study is an extension of previously reported investigations into CNT/alumina epoxy nanocomposites. A series of epoxy composites with different CNT/alumina loadings were investigated with regard to their thermal-degradation kinetics and lifetime prediction. The thermal-degradation parameters were acquired via thermogravimetric analysis (TGA) in a nitrogen atmosphere. The degradation activation energy was determined using the Flynn–Wall–Ozawa (F-W-O) method for the chosen apparent activation energy. The Ea showed significant differences at $\alpha > 0.6$, which indicate the role played by the CNT/alumina hybrid filler loading in the degradation behavior. From the calculations, the lifetime prediction at 5% mass loss decreased with an increase in the temperature service of nitrogen. The increase in the CNT/alumina hybrid loading revealed its contribution towards thermal degradation and stability. On average, a higher Ea was attributed to greater loadings of the CNT/alumina hybrid in the composites.

Keywords: CNT hybrid; alumina; epoxy; kinetic; activation energy; lifetime

Citation: Kudus, M.H.A.; Zakaria, M.R.; Omar, M.F.; Hafi Othman, M.B.; Md. Akil, H.; Nabiałek, M.; Jeż, B.; Abdullah, M.M.A.B. Nonisothermal Kinetic Degradation of Hybrid CNT/Alumina Epoxy Nanocomposites. *Metals* **2021**, *11*, 657. https://doi.org/10.3390/met11040657

Academic Editor: Emin Bayraktar

Received: 21 February 2021
Accepted: 15 April 2021
Published: 17 April 2021

1. Introduction

Hybrid polymer nanocomposites are becoming popular due to their unique combination of properties, which are not possible when a single filler system is used. In the past, several researchers demonstrated that the combination of properties could be achieved by combining two or more different types of fillers [1–4]. The synthesis of a CNT/alumina hybrid compound has been reported in previous works [5–7], where its composites demonstrated good mechanical and thermal properties [8]. It is a well-known fact that CNTs possess great mechanical, thermal, electrical, and chemical properties, and can be used in polymer composites due to their unique structure [9–12]. However, their lack of dispersibility in a polymer matrix and their tendency to agglomerate with each other always hinder their original performance. It has been agreed upon by researchers worldwide that CNT is not capable of being easily dispersed in a polymer resin, even by using advance ultrasonication techniques. Various studies of functionalization techniques

for CNTs have been carried out in the past to achieve a dispersible CNT in a polymer matrix [13,14]. Note that alumina particles have been found to have very dispersible properties in a polymer matrix, either in simple conventional stirring or advanced ultrasonication techniques. [15,16]. The idea of hybridization between CNTs and alumina is the growing of CNTs homogenously onto alumina particles, and alumina acting as vehicle to assist the dispersion of CNTs through the epoxy matrix. Many studies have been carried out to obtain well-dispersed fillers in nanocomposite applications, such as surface modification [17–19], chemical functionalization [20–22], and hybridization on the particulate fillers [23–25]. Based on our previous study, at CNT/alumina hybrid loading of 3 wt%, the tensile strength and modulus increased by about 30% to 39%, while the flexural strength and modulus increased by between 30% and 35%, and the dielectric constant increased by about 20%. Meanwhile, the thermal conductivity increased by about 30% at 5 wt% of CNT/alumina hybrid loading [8].

Additionally, the contribution toward kinetic degradation and thermal stability as a result of different CNT/alumina loadings on the lifetime of the epoxy system has not been well explored. The information about kinetic degradation and in-use lifetime projections can be obtained experimentally. The ability to predict the lifetime is valuable because the cost of premature failure in actual end use can be high [26]. Thermogravimetric analysis (TGA) provides a method for accelerating the lifetime testing of polymers so that short-term experiments can be used to predict in-use lifetime [27]. The lifetime is considered when 5% mass loss is reached from a dynamic thermogravimetric analysis [28]. Thus, this paper seeks to provide a few insights on the basic investigation of kinetic degradation using multiple heating rate methods (nonisothermal) like the Flynn–Wall–Ozawa method. It was found to be more convenient to carry out nonisothermal runs because it was not necessary to induce a sudden temperature jump in the sample at the beginning. The kinetic degradation and glass transition, as well as the chain mobility, can be derived and generate parameters that are subsequently used to deduce the lifetime of a polymer at different temperatures. The thermal behavior of an epoxy system has been reported to depend on the polymeric network crosslink density, functional group, types of curing agents [29], and filler properties [30,31]. However, the thermal-degradation kinetic study of an epoxy with a hybrid filler system has been less-reported previously. Besides that, different filler loadings will generate different thermal characteristics due to the thermal flow path connecting each filler particle, as well as the homogeneous distribution of the filler [32,33].

The present paper deals with the comparative nonisothermal degradation kinetics of different CNT/alumina hybrid filler loadings in epoxy nanocomposites. The apparent activation energy was determined using the Flynn–Wall–Ozawa, Kissinger, and Coats-Redfern methods. The data presented in this study will be very useful for qualitatively or quantitatively estimating and distinguishing the lifetime of an epoxy system. In addition, the objective of this study was to link the methods that were previously studied in isolation by reviewing them together, as well as to provide useful information on a wide range of related areas. The type of solid-state mechanism was determined by the Criado method using Flynn–Wall–Ozawa kinetic data at low conversion based on Doyle's approximation. The kinetic parameters (rate constant, k; activation energy, Ea) were calculated and subsequently employed to predict the influence of different CNT/alumina loadings on the lifetime.

2. Materials and Methods

2.1. Materials

Bisphenol A diglycidyl ether (DGEBA) and trimethylhexamethylenediamine (TMD) were purchased from Eurochemo Pharma Sdn. Bhd. A CNT/alumina hybrid compound was synthesized via CVD and used as the composite filler in an epoxy composite [34].

2.2. Fabrication of CNT/Alumina Epoxy Nanocomposites

The epoxy composites were prepared by mixing the epoxy resin with an amount of CNT/alumina compound. The mixture was stirred for 30 min and then subjected to high frequency sonication for 10 min. After that, a hardener, TMD, was added to the mixture, and it was then stirred accordingly. The final mixture was then degassed in a vacuum for 1 h in order to remove bubbles and trapped air. The mixture was poured into the desired molds and cured at 120 °C for 1 h. The preparation of the epoxy nanocomposite samples is summarized in Table 1, while the details have been reported elsewhere [8].

Table 1. Summary of preparation of epoxy nanocomposite samples.

Samples	DGEBA:TMD	CNT/Alumina (wt%)	Curing (Temperature, Time)
Epoxy00	10:6	0	120 °C, 1 h
Epoxy/HYB1	10:6	1	120 °C, 1 h
Epoxy/HYB3	10:6	3	120 °C, 1 h
Epoxy/HYB5	10:6	5	120 °C, 1 h

2.3. Characterizations

The morphological images of the CNT/alumina epoxy nanocomposites were obtained with a field emission scanning electron microscope (FESEM) (ZESS Supra 35 VP, Germany) and a higher-resolution transition electron microscope (HTEM) Philips TECNAI 20, Germany.

2.4. Thermal Analysis

The dynamic and nonisothermal thermogravimetric analyses were conducted using a Mettler Toledo thermogravimetric analyzer. About 10 mg of the sample was placed in an aluminum crucible and heated from a temperature of 50 °C to 800 °C at heating rates of 5, 10, and 20 °C min^{-1} in a nitrogen atmosphere purge. The mass loss versus the temperature was recorded. The onset decomposition temperature (Td), 10% mass loss temperature (T10), and residual mass (Rw) at 800 °C were also determined. Finally, a kinetic analysis via the Flynn–Wall–Ozawa method was carried out at three heating rates, i.e., 5, 10, and 20 °C min^{-1}. The type of solid-state mechanism was determined by the Criado method using Flynn–Wall–Ozawa kinetic data at a low conversion ($\alpha < 30\%$) based on Doyle's approximation.

3. Results

3.1. Characteristics and Morphology of the CNT/Alumina

In this study, a CNT/alumina hybrid compound (HYB) was used as the filler in an epoxy system and was investigated with a series of filler loadings. Figure 1 shows the HRTEM images of the CNT/alumina hybrid in the epoxy/HYB composites [7]. The images show that the CNT and alumina were attached to each other even though they were subjected to high-frequency sonication during the fabrication of the composite.

The thermal stability of the CNT/alumina epoxy composites was evaluated using TGA in a nitrogen atmosphere at heating rates of 5, 10, and 20 °C min^{-1}. The mass residue versus the temperature curve of the thermal degradation for the composites based on the corresponding filler loadings at different heating rates are shown in Figure 2.

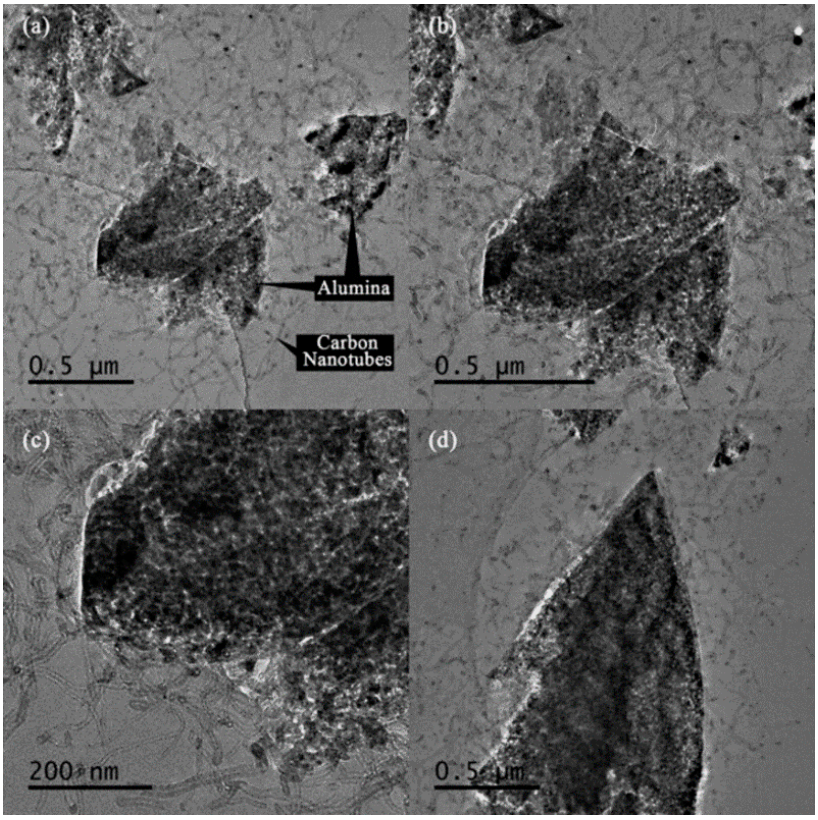

Figure 1. HRTEM images of CNT/alumina hybrid in epoxy composites [7] at different magnifications. (**a**) 9900×; (**b**) 15,000×; (**c**) 29,000×; (**d**) 12,000×.

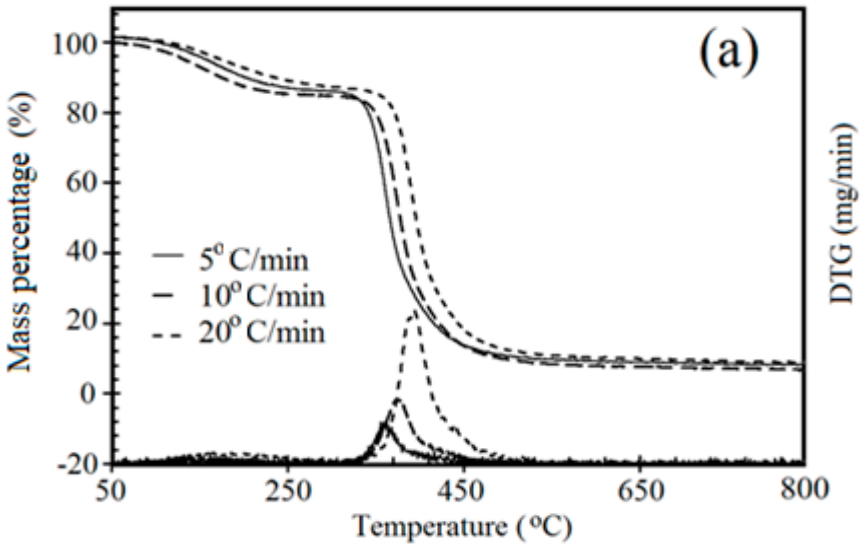

Figure 2. *Cont.*

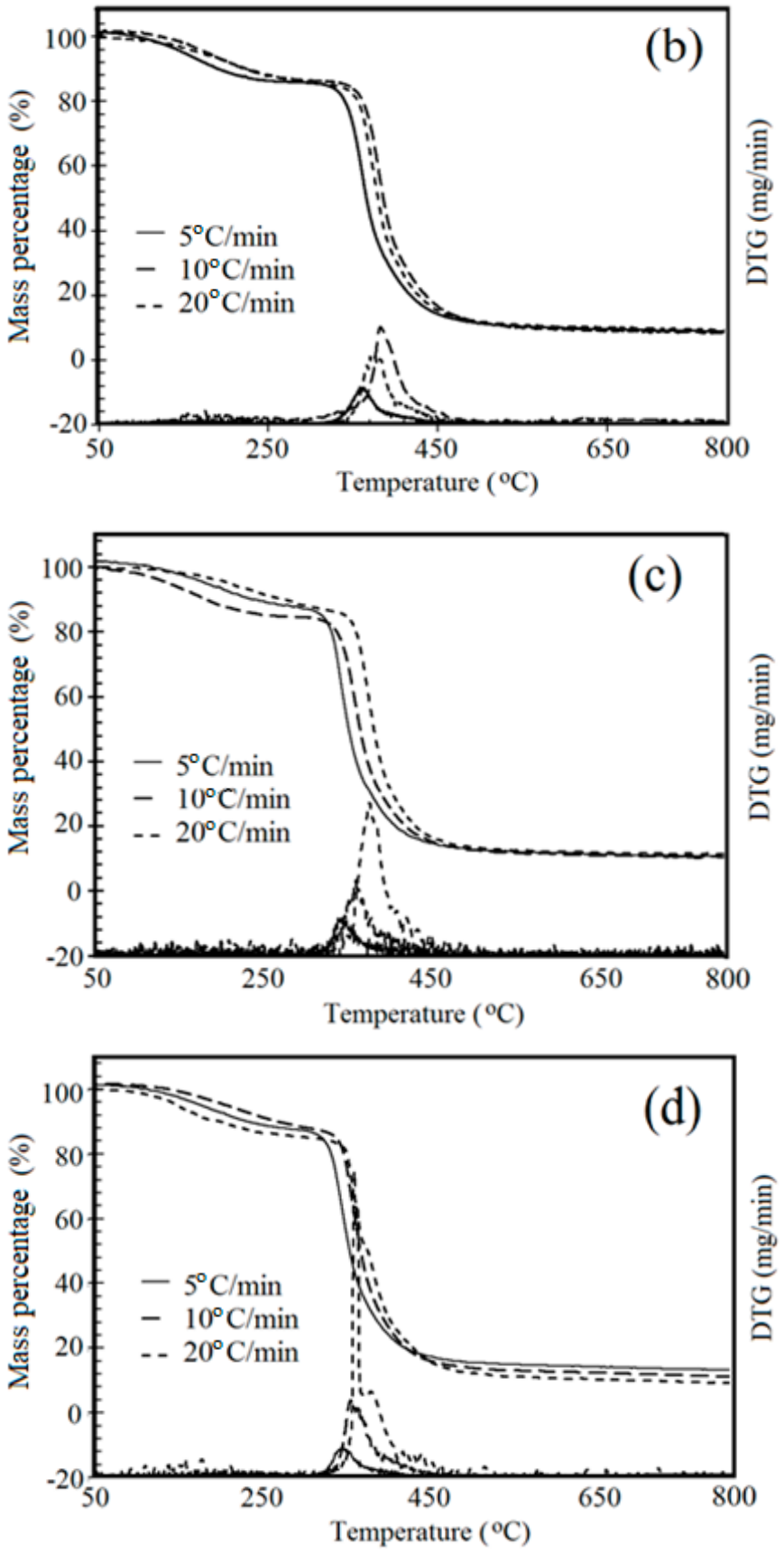

Figure 2. Variation of mass residue versus temperature at different heating rates of epoxy composites with (**a**) no filler, (**b**) 1% MWCNT/alumina, (**c**) 3% MWCNT/alumina, and (**d**) 5% MWCNT/alumina.

Figure 2a–d show that major decomposition occurred at 400 °C, with more than 10% residue once the degradation was completed at 800 °C. The curve was delayed and shifted to the higher temperatures as the heating rate was increased from 5 to 20 °C min^{-1}. From Figure 2a–c, it is evident that the thermal decomposition of the sample proceeded in the range of 100–800 °C. The TG curve pattern demonstrated two stages in the thermal-decomposition temperature. The first thermal event occurred in the range of 50–250 °C, corresponding to the evaporation of the bound water and air bubbles, while the second thermal event occurred in the range of 300–450 °C, corresponding to further breakage of the bond links, main chain scission, and dehydration.

Meanwhile, as a comparison, the thermal degradation of epoxy-based composites corresponding to the same heating rates among different filler loadings are shown in Figure 3. Although the curves in Figure 3a–c do not show any significant change with a change in filler loadings, but it is clear that the curves displayed do not overlap. This proves that the filler loading played a role, although not a large one, in stability during thermal degradation.

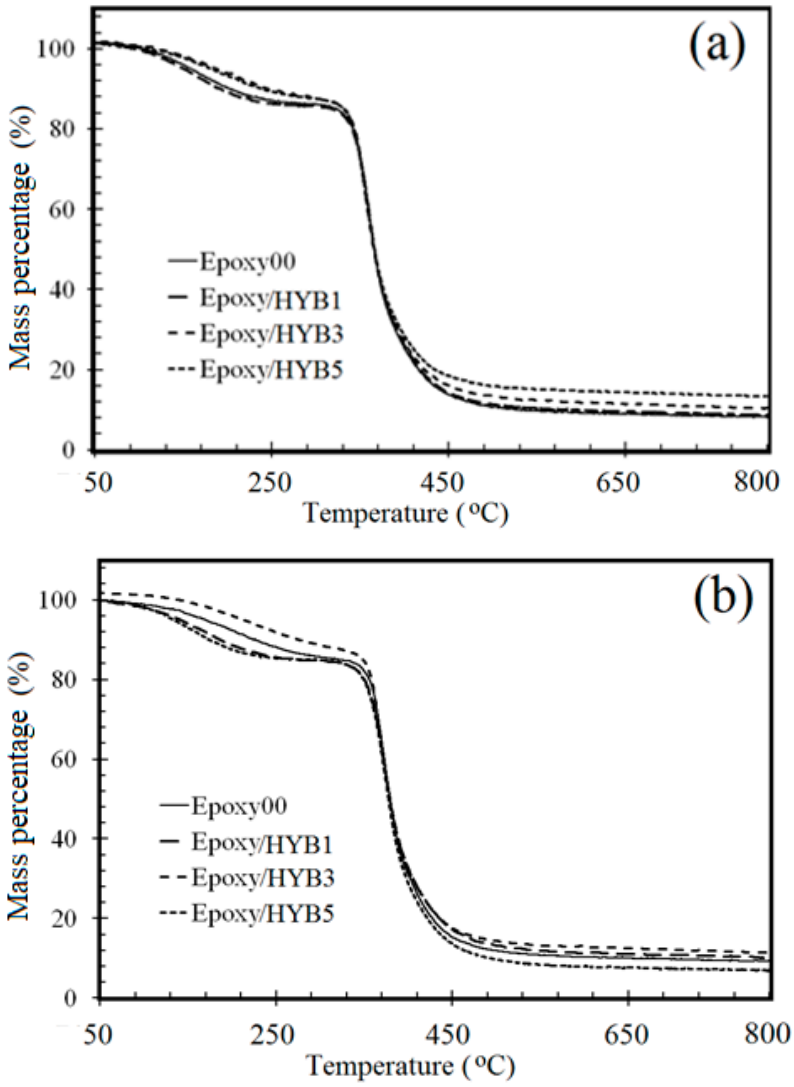

Figure 3. *Cont.*

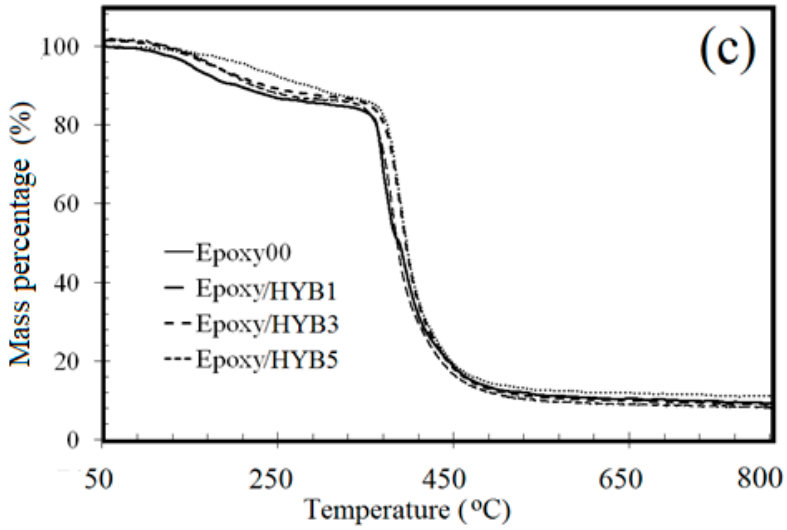

Figure 3. Comparison of mass residue for epoxy composites with different filler loading at (**a**) β = 5 °C min^{-1}, (**b**) β = 10 °C min^{-1}, and (**c**) β = 20 °C min^{-1}.

The curves in Figure 3 showed significant changes of temperature at the maximum rate of mass residue with increased filler loadings, and it was clear that the increment in the filler loadings contributed to the thermal stability of the composites during thermal degradation. The char yield of the Epoxy00 with no filler at 600 °C showed the least mass percentage, followed by the char yield of Epoxy/HYB1, Epoxy/HYB3, and Epoxy/HYB5. Hence, this reflected the amount of filler that was not degraded thermally at the current temperature. Thus, the kinetic parameters could be reasonably evaluated here. Table 2 summarizes the TG trace of the CNT/alumina hybrid epoxy composites in a nitrogen atmosphere.

Table 2. Result of TG/DTG traces of some epoxy nanocomposites in a nitrogen atmosphere.

Samples	β	Char Residue [a]	$T_{10\%}$ (°C) [e]	T_{onset} (°C) [b]	T_{max} (°C) [c]	T_{end} (°C) [d]	ΔT (°C) [f]
Epoxy00	5	8.23	201.5	320.18	360.42	522.83	202.65
	10	7.38	209.5	328.12	377.42	529.70	201.58
	20	8.97	218.0	355.50	394.90	596.00	240.50
	Average	8.19	209.66	343.50	376.43	565.50	222.00
Epoxy/HYB1	5	9.24	190.35	320.80	362.80	583.80	263.00
	10	10.79	216.80	341.10	373.40	556.40	215.30
	20	8.91	230.60	332.90	382.50	497.80	164.90
	Average	9.65	209.10	331.60	372.90	546.00	214.40
Epoxy/HYB3	5	10.94	239.10	326.50	351.40	502.10	175.60
	10	12.14	186.04	340.00	373.70	589.70	249.70
	20	10.31	272.00	351.20	391.70	601.00	249.80
	Average	11.13	230.00	339.23	372.27	564.27	225.03
Epoxy/HYB5	5	13.9	247.50	325.60	357.20	494.50	168.90
	10	12.15	257.80	345.60	366.60	556.70	211.10
	20	11.73	213.00	347.80	371.90	603.60	255.80
	Average	12.59	239.43	339.67	365.23	551.60	211.93

[a] Wt% residue at 800 °C; [b] onset temperature of degradation; [c] temperature of maximum rate of mass loss; [d] end temperature of degradation; [e] temperature corresponding to percentage of mass loss; [f] $\Delta T = T_{end} - T_{onset}$.

Three ways in which a material is able to lose mass during heating are through the release of adsorbed species, chemical reactions, and decomposition. All of these show that the material is no longer thermally stable. From Table 3, the kinetic stability of the

epoxy/HYB composites were determined by observing $T_{10\%}$, the temperature at 10% of reduced mass. The average of $T_{10\%}$ increased slightly with a corresponding increase in the filler loading. The significant improvement in thermal stability could be attributed to the combination of CNT and alumina in the HYB structure, which introduced a pathway for the heat transfer [8]. The higher amount of HYB contributed to a more tortuous pathway for the heat transfer. The efficiency of the heat transfer dissipated the heat and delayed the chain-scission process.

Table 3. Activation energies at $\alpha < 30$ obtained by using the Flynn–Wall–Ozawa method.

α	Ea ($kJmol^{-1}$)	R^2	α	Ea ($kJmol^{-1}$)	R^2
	Epoxy00			Epoxy/HYB1	
0.05	84.31	0.8820	0.05	100.76	0.8031
0.10	98.83	0.9317	0.10	112.05	0.8900
0.15	127.94	0.8114	0.15	141.32	0.9394
0.20	137.55	0.9375	0.20	163.22	0.9900
0.25	144.79	0.9654	0.25	210.65	0.9902
0.30	149.40	0.9770	0.30	212.36	0.9392
Average	123.80	-	Average	156.73	-
	Epoxy/HYB3			Epoxy/HYB5	
0.05	79.81	0.8768	0.05	76.51	0.8390
0.10	92.48	0.8381	0.10	88.48	0.8012
0.15	117.13	0.8371	0.15	112.28	0.8926
0.20	129.32	0.9073	0.20	147.40	0.8393
0.25	139.62	0.9681	0.25	173.57	0.8613
0.30	142.04	0.9876	0.30	219.75	0.8797
Average	116.73	-	Average	136.33	-

The average char residue for all the samples was less than 20% once the degradation was completed at 600 °C. The higher loading of HYB in the epoxy composites resulted in a higher char residue from 50 °C to 800 °C, suggesting that epoxy composites with higher HYB loadings have better thermal stability than epoxy composites with lower amounts of HYB filler. The char yield of epoxy/HYB increased with an increase in the HYB content, indicating that the composites were thermally stable at high temperatures. Owing to the thermal stability of alumina, the hybrid combination of CNT and alumina in the HYB filler exhibited synergic thermal absorption and dissipation, whereby the CNT and alumina could absorb part of the heat, thus forming the barrier effect of fillers. This enhanced the resistance to thermal degradation, prevented the diffusion of the decomposition products from the epoxy into the gas phase, and delayed the thermal-degradation process. Wang et al. discussed the thermal-absorption ability of constituents in epoxy composites that provide the resistance to thermal degradation [35].

3.2. Calculation of Thermal Degradation Kinetic Parameters

Generally, in the kinetics of polymer degradation, it is assumed that the rate of conversion (α) is proportional to the concentration of the reacted material. In our case, an α here is representative of the degradation of hybrid CNT/alumina epoxy nanocomposites in a nitrogen atmosphere. Thus, the rate of conversion can be expressed by the following basic rate equation (Equation (1)):

$$\frac{d\alpha}{dt} = k(T)f(\alpha) \quad (1)$$

where $d\alpha/dt$ is the conversion rate, k is the rate constant, and $f(\alpha)$ is a function of the conversion. However, in cases of thermogravimetric analysis, the fraction concentration of the reacted material (α) is represented as a total mass loss of the complete degradation process. Thus means, the conversion α can be calculated as Equation (2):

$$\alpha = \frac{M_o - M_t}{M_o - M_f} \tag{2}$$

where M_o, M_t, and M_f, are the initial mass of the hybrid CNT/alumina epoxy nanocomposites at 50 °C, the mass of the hybrid CNT/alumina epoxy nanocomposites at 50 °C at all temperatures, and the final mass hybrid CNT/alumina epoxy nanocomposites at 800 °C, respectively, of the completely decomposed sample. According to the Arrhenius equation (Equation (3)), k is given by:

$$k = A\ \exp -\frac{Ea}{RT} \tag{3}$$

where A is the frequency factor, Ea is the apparent kinetic energy of the degradation reaction, R is the gas constant, α is the conversion, and T is the absolute temperature. It can be assumed that k, from Equation (1), follows the Arrhenius equation. Thus, by substituting Equation (3) into Equation (1), Equation (4) is obtained:

$$\frac{\mathrm{d}\alpha}{\mathrm{d}t} = A \exp\left(-\frac{Ea}{RT}\right) f(\alpha) \tag{4}$$

According to non-isothermal kinetic theory, thermal degradation data is generally performed by Equation (5):

$$\frac{\mathrm{d}\alpha}{\mathrm{d}t} = \beta\frac{d\alpha}{dT} = A \exp\left(-\frac{Ea}{RT}\right) f(\alpha) \tag{5}$$

where $\beta = dT/dt$ is the constant heating rate. Equation (5) can be rearranged in order to be simplified as Equation (6):

$$\frac{\mathrm{d}\alpha}{\mathrm{d}t} = \frac{A}{\beta} \exp(-\frac{Ea}{RT}) f(\alpha) \tag{6}$$

where $f(\alpha)$ is the differential expression of a kinetic model function; a is the conversion; β is the heating rate (K/min); Ea and A are the activation energy (kJ/mol) and the pre-exponential factor (min^{-1}), respectively, for the decomposition reaction; and R is the gas constant (8.314 $Jmol^{-1}$ K^{-1}). Generally, Ea can be calculated by using the Flynn–Wall–Ozawa, Kissinger, Coats–Redfern, Horowitz–Metzger, MacCallum–Tanner, or van Krevelen methods. However, the Flynn–Wall–Ozawa method is one of the superior methods for dynamic heating experiments, as the calculation of Ea does not take the reaction order into account. Thus, this method was taken into consideration in the discussion.

The Flynn–Wall–Ozawa method can be used to quantify Ea without any knowledge of the reaction mechanism. This is not based on any assumption concerning the temperature integral, thus giving a higher degree of precision to the results. Thus, this method is a free model technique that evaluates the dependence of the effective activation energy on conversion. Besides that, this method is very useful for the kinetic interpretation of TG data obtained from complex reactions. From Equation (6), it can be integrated using the Doyle approximation [36]. The result of the integration after considering the logarithms was Equation (7) or Equation (8):

$$\log \beta = \log \frac{AE_a}{g(\alpha)R} - 2.315 - \frac{0.457E_a}{RT} \tag{7}$$

or

$$\ln \beta = \ln\left(\frac{AE_a}{R}\right) - \ln g(\alpha) - 5.3305 - \frac{1.052E_a}{RT} \tag{8}$$

where the Ea of the thermal degradation process of the blending system was determined from the slope of the straight-line log β versus $1/T$.

The Ea of the different filler loadings of the CNT/alumina epoxy nanocomposites was determined from a linear fitting of log β versus $1000/T$ at different conversions. To apply the iso-conversional F–W–O method from Equation (7), the thermal decomposition of each

filler loading was scanned at different βs: α = 0.1 and α = 0.9 were taken at 100 °C and 800 °C, respectively. The *Ea* of different filler loadings of the epoxy nanocomposites was determined from the slope of the linear fitting of log β versus $1000/T$ at different values of α (Figure 4a–d).

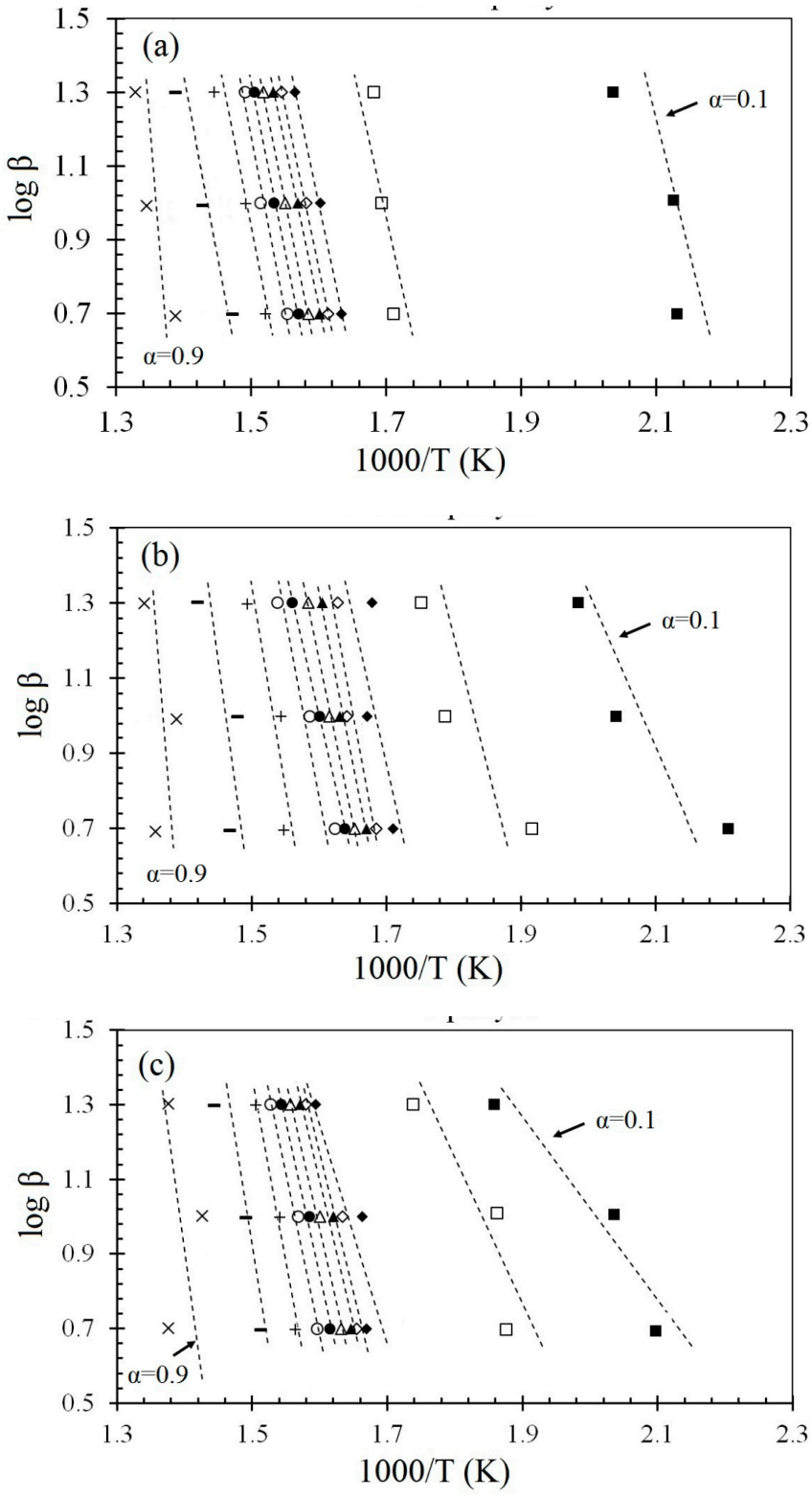

Figure 4. *Cont.*

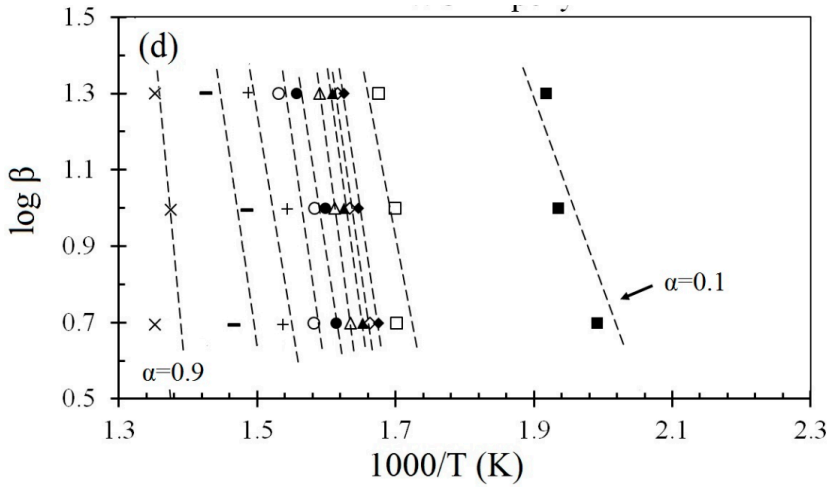

Figure 4. Plot of log β versus 1000/T at different heating rates according to the Flynn–Wall–Ozawa method at different conversion [x = 0.9, - = 0.8, + = 0.7, o = 0.6, ● = 0.5, Δ = 0.4, ▲ = 0.3, ◊ = 0.25, ♦ = 0.2, □ = 0.15, ■ = 0.1] for (**a**) Epoxy00, (**b**) Epoxy/HYB1, (**c**) Epoxy/HYB, and (**d**) Epoxy/HYB5.

The *Ea* values corresponding to the different conversions using the Flynn–Wall–Ozawa method are listed in Table 3. The *Ea* values calculated from using this method were 123.80, 156.73, 116.73, and 136.33 kJ/mol for Epoxy00, Epoxy/HYB1, Epoxy/HYB3, and Epoxy/HYB5, respectively.

From Figure 4a–d of the plot of log β versus 1000/T at different βs, it was found that a negative *Ea* was obtained from the gradient, and it was revealed that the best-fitting straight lines were nearly parallel for various heating rates and different samples. By following an approximately exponential relationship so that the rate constant could still be fitted to an Arrhenius expression, a negative value of *Ea* was obtained. This means that the rates of degradation decreased with an increase in temperature. Further increases in temperature led to a reduced probability of the colliding molecules capturing one another. The summary and comparison of the epoxy nanocomposites *Ea* derived from different filler loadings are shown in Figure 5.

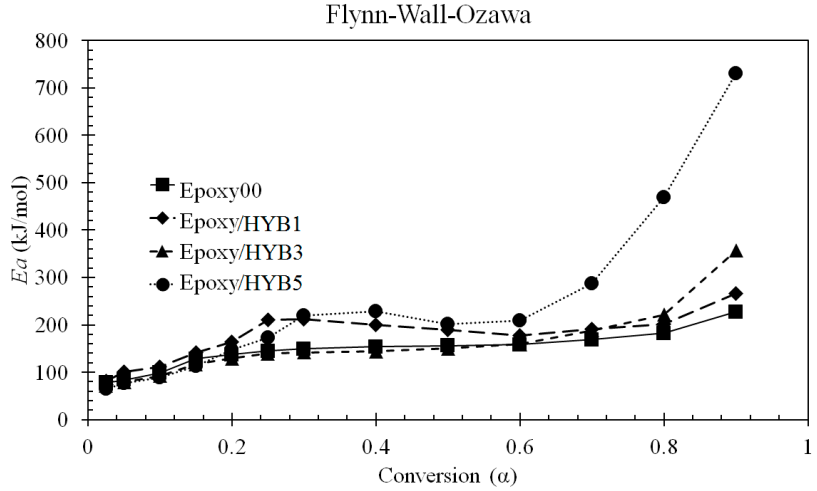

Figure 5. Comparison of *Ea* versus conversion corresponding to different filler loadings using the Flynn–Wall–Ozawa method.

Figure 5 shows the plot with a constant E_a, which is clearly indicated by the presence of a multistep process. However, in this study, two stages of E_a were determined, where the first stage of the E_a behavior occurred at $\alpha < 0.6$ and the second stage started at $\alpha > 0.6$. In the first stage, the E_a increased moderately throughout the degradation process. In this

stage, the degradation kinetics were associated with the breakage of weak links. According to Neĭman et al., the thermal degradation of a hardened epoxy system within a lower temperature range (300–450 °C) produces H_2, CO, CH_4, C_2H_6, C_2H_4, C_3H_6, and C_3H_8 [37] as a result of the breakage of weaker bonds. The works of Norman Grassie et al. showed that at 300 °C the principal products are small amounts of hydrogen and methane, ethane, propene, ammonia, methylamine with a trace of trimethylamine, water, phenol, cresols, 4-isopropyl phenol, 4-isopropenyl phenol, bisphenol-A, 2-(benzo-fur-5-yl)-2-(p-hydroxy phenyl)propane, and 2-(benzo-pyran-6-yl)-2-(p-hydroxy phenyl)propane [38,39].

Generally, in this study, the degradation was probably due to the breakdown of the aliphatic segment of the epoxy (C-$(CH_3)_2$) from the DGEBA units, or it could also be attributed to the weak bonds that might have existed (-NH-and -CONH-) between the side-chain substituents, which are the weakest linkages along the main chain of the polymer. At the second stage, once $\alpha > 0.6$ and as these weak links were consumed, the limiting step of degradation shifted toward the degradation initiated by random scission. This type of degradation requires higher levels of energy. The energy to break the CNT and alumina structures was parallel to the increment in the filler loading, which resulted in the E_a trend.

There is a relationship between the degradation behavior of the samples and the corresponding activation energy required to initiate the thermal-degradation process with increases in the CNT/alumina content in the epoxy composites. The Epoxy/HYB5 sample with 5 wt% filler loading demonstrated the highest *Ea*, followed by the Epoxy/HYB3, Epoxy/HYB1, and Epoxy00 samples with 3 wt%, 1 wt%, and no filler, respectively. This distinction can be explained by comparing the bond-dissociation energy between the hybrid fillers (ΔH° Al-C = +267.7 kJmol^{-1}) among the CNT (ΔH° C=C = +618.3 kJmol^{-1}) and alumina constituents Al-O (ΔH° Al-O = +501.9 kJmol^{-1}). Since an increase in the filler loading meant a reduction in the DGEBA/TMD volume fraction and an increase in the CNT/alumina volume fraction, the high *Ea* at higher conversion therefore corresponded to the filler amount.

3.3. Lifetime Predictions

Lifetime estimations are also very useful in the development, design, and selection of polymers for different applications. The apparent kinetic parameters calculated from this study were used to arrive at the lifetime of the formulated epoxy systems. The estimated lifetime of an epoxy composite until failure has been defined as the time when the mass loss reaches 5 wt% ($\alpha = 0.05$) [40–42]. Lifetime can be estimated from the integration of Equation (9):

$$\frac{d\alpha}{dt} = A \exp \frac{Ea}{RT}(1-\alpha)^n \tag{9}$$

From the from the integration of Equation (9), estimated lifetime equal to Equation (10) for the reaction order $n \neq 1$, and Equation (11) for the reaction order $n \neq 1$.

$$t_f = \frac{(1-0.95^{1-n})}{A(1-n)} \exp \frac{Ea}{RT} \ (\mathrm{n} \neq 1) \tag{10}$$

$$t_f = \frac{0.0513}{A} \exp \frac{Ea}{RT} \ (\mathrm{n} = 1) \tag{11}$$

The value of the reaction order (n) can be obtained directly from the symmetrical index of a DTG peak, based on the second Kissinger technique, as demonstrated in Equation (12):

$$n = 1.88 \frac{\left[\frac{d^2\alpha}{dt^2}\right]_L}{\left[\frac{d^2\alpha}{dt^2}\right]_R} \tag{12}$$

where the indices L and R correspond to the left and right peak ($d^2\alpha/dt^2$) values on the second derivative thermogravimetric (DDTG) curve for the decomposition process, respectively. Using the kinetic data and Equation (4), the estimated value of the lifetime in a

nitrogen and air atmosphere at a mass loss of 5 wt% at various temperatures are presented in Figure 6, and the *n* and ln A values for the decomposition in a nitrogen atmosphere are listed in Table 4.

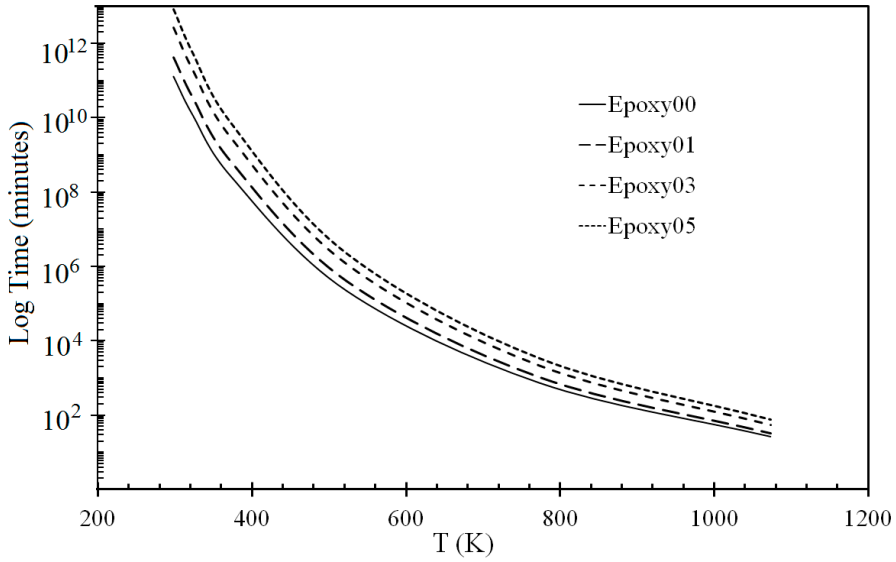

Figure 6. Lifetime prediction.

Table 4. Result of kinetic-degradation parameter and lifetime as a function of service temperature in the presence of the type of silicone segment in a nitrogen atmosphere.

Sample Designation	n [a]	Ea	ln A [b]	Lifetime Predictions [c]					
				25 °C	50 °C	100 °C	150 °C	250 °C	500 °C
Epoxy00	0.9	76.51	2.33	11.11	10.07	8.41	5.34	2.87	1.42
Epoxy01	0.9	79.81	2.37	11.67	10.59	8.86	5.65	3.07	1.56
Epoxy03	0.9	84.31	2.47	12.42	11.27	9.44	6.06	3.33	1.74
Epoxy05	0.9	87.14	2.48	12.91	11.72	9.84	6.33	3.52	1.86

[a] Kinetic order; [b] pre-exponential factor; [c] lifetime predictions of service temperature.

In a nitrogen atmosphere, the lifetime predicted for all epoxy composite systems assumes pseudo-first-order reaction kinetics with an exponential curve. It can be seen that the lifetime was strongly dependent on the service temperature, and significantly decreased from 300 °C to 600 °C, while an increase in the rate of degradation shortened the lifetime. The lifetime difference between each epoxy composite was quite small and exhibited the same pattern.

From Figure 6, it can be seen that the lifetime curves achieved the same pattern due to the same epoxy-system base. The difference was only on $t_{1/2}$ of the epoxy composites. The $t_{1/2}$ of the neat epoxy (Epoxy00) was lower than the $t_{1/2}$ of the epoxy with 1% CNT/alumina hybrid (Epoxy/HYB1) due to the dissociation energy of the chemical bonding in Epoxy00 and Epoxy/HYB1. The Epoxy/HYB1 contained a lower proportion of epoxy but an extra proportion of filler. A lower epoxy proportion means less weak chemical bonding, while the presence of the CNT/alumina filler proportion increased the *Ea* needed to break the stronger bonds. The Epoxy/HYB3 and Epoxy/HYB5 possessed a lower proportion of epoxy and a greater amount of CNT/alumina, as explained by the curve patterns. Hence, increasing the filler loading led to increases in the *Ea* and $t_{1/2}$.

4. Conclusions

The results of the thermogravimetric analysis of composite materials based on an epoxy system containing 1% to 5% of CNT/alumina hybrid reinforcement were presented

in this work. The decomposition of the samples took place in the first major step, followed by a second smaller step. The initial decomposition temperature was established between 50 and 250 °C. The major decomposition took place from 250 to 450 °C. The increasing heating rate simultaneously moved the plots toward higher temperatures. The results obtained from the thermogravimetric analysis were used to calculate the activation energy by means of nonisothermal methods. The lifetime of the epoxy CNT/alumina hybrid composites was estimated by increasing the temperature service in nitrogen.

Author Contributions: Conceptualization, M.M.A.B.A.; methodology, M.B.H.O., M.H.A.K., H.M.A. and M.R.Z.; formal analysis, M.B.H.O., M.R.Z. and M.F.O.; investigation, M.B.H.O. and M.R.Z.; writing—original draft preparation, M.R.Z. and M.H.A.K.; writing—review and editing, M.N. and B.J. All authors have read and agreed to the published version of the manuscript.

Funding: This research was funded by Universiti Sains Malaysia through RUI 1001/PBAHAN/8014047 and USM-STG-6315076.

Institutional Review Board Statement: Not applicable.

Informed Consent Statement: Not applicable.

Data Availability Statement: Not applicable.

Acknowledgments: The authors wish to acknowledge the School of Chemical Sciences and School of Mechanical Engineering, Universiti Sains Malaysia and Faculty of Chemical Engineering Technology, Universiti Malaysia Perlis for sponsoring postdoctoral fellowship.

Conflicts of Interest: The authors declare no conflict of interest.

Abbreviations

CNT	carbon nanotube
HYB	CNT/alumina hybrid compound
DGEBA	Bisphenol A diglycidyl
TMD	Trimethylhexamethylenediamine
α	Conversion
log β	Heating rate; ($Kmin^{-1}$)
$d\alpha/dt$	Rate of conversion
$d^2\alpha/dt^2$	Rate of conversion for second-derivative thermogravimetry
f(α)	Expression of kinetic model
Ea	Activation energy
Eq	Equation
F–W–O	Flynn–Wall–Ozawa
k	Rate constant
M_o	Initial mass (g)
M_t	Mass at time (g)
M_f	Final mass (g)
n	Kinetic order
N_2	Nitrogen
T_5	Temperature at 5% mass loss (K)
T_{10}	Temperature at maximum mass loss (K)
PEPA	Polyethylene polyamine
R	Gas constant (8.1 $Jmol^{-1}$ K^{-1})
R_w	Residue mass (g)
T_d	Temperature at maximum mass loss (K)
TG	Thermogravimetry (TG)
T_g	Glass transition temperature
T	Temperature (K)
t	Time (min)

References

1. He, D.; Fan, B.; Zhao, H.; Yang, M.; Wang, H.; Bai, J.; Li, W.; Zhou, X.; Bai, J. Multifunctional polymer composites reinforced by carbon nanotubes–Alumina hybrids with urchin-like structure. *Mater. Today Commun.* **2017**, *11*, 94–102. [CrossRef]
2. Yan, R.; Su, F.; Zhang, L.; Li, C. Highly enhanced thermal conductivity of epoxy composites by constructing dense thermal conductive network with combination of alumina and carbon nanotubes. *Compos. Part A Appl. Sci. Manuf.* **2019**, *125*, 105496. [CrossRef]
3. Liu, Y.; He, D.; Dubrunfaut, O.; Zhang, A.; Zhang, H.; Pichon, L.; Bai, J. GO-CNTs hybrids reinforced epoxy composites with porous structure as microwave absorbers. *Compos. Sci. Technol.* **2020**, *200*, 108450. [CrossRef]
4. Wilkinson, A.N.; Kinloch, I.A.; Othman, R.N. Low viscosity processing using hybrid CNT-coated silica particles to form electrically conductive epoxy resin composites. *Polymer* **2016**, *98*, 32–38. [CrossRef]
5. Zakaria, M.R.; Akil, H.M.; Abdul Kudus, M.H.; Othman, M.B.H. Compressive properties and thermal stability of hybrid carbon nanotube-alumina filled epoxy nanocomposites. *Compos. Part B Eng.* **2016**, *91*, 235–242. [CrossRef]
6. Zakaria, M.R.; Abdul Kudus, M.H.; Md. Akil, H.; Zamri, M.H. Improvement of Fracture Toughness in Epoxy Nanocomposites through Chemical Hybridization of Carbon Nanotubes and Alumina. *Materials* **2017**, *10*, 301. [CrossRef] [PubMed]
7. Zakaria, M.R.; Md. Akil, H.; Abdul Kudus, M.H.; Kadarman, A.H. Improving flexural and dielectric properties of MWCNT/epoxy nanocomposites by introducing advanced hybrid filler system. *Compos. Struct.* **2015**, *132*, 50–64. [CrossRef]
8. Zakaria, M.R.; Akil, H.M.; Kudus, M.H.A.; Saleh, S.S.M. Enhancement of tensile and thermal properties of epoxy nanocomposites through chemical hybridization of carbon nanotubes and alumina. *Compos. Part A Appl. Sci. Manuf.* **2014**, *66*, 109–116. [CrossRef]
9. Shin, J.; Lee, K.; Jung, Y.; Park, B.; Yang, S.J.; Kim, T.; Lee, S.B. Mechanical Properties and Epoxy Resin Infiltration Behavior of Carbon-Nanotube-Fiber-Based Single-Fiber Composites. *Materials* **2021**, *14*, 106. [CrossRef]
10. Guo, H.; Ji, P.; Halász, I.Z.; Pirityi, D.Z.; Bárány, T.; Xu, Z.; Zheng, L.; Zhang, L.; Liu, L.; Wen, S. Enhanced Fatigue and Durability Properties of Natural Rubber Composites Reinforced with Carbon Nanotubes and Graphene Oxide. *Materials* **2020**, *13*, 5746. [CrossRef]
11. Rizzo, A.; Luhrs, C.; Earp, B.; Grbovic, D. CNT Conductive Epoxy Composite Metamaterials: Design, Fabrication, and Characterization. *Materials* **2020**, *13*, 4749. [CrossRef]
12. Trakakis, G.; Tomara, G.; Datsyuk, V.; Sygellou, L.; Bakolas, A.; Tasis, D.; Parthenios, J.; Krontiras, C.; Georga, S.; Galiotis, C.; et al. Mechanical, Electrical, and Thermal Properties of Carbon Nanotube Buckypapers/Epoxy Nanocomposites Produced by Oxidized and Epoxidized Nanotubes. *Materials* **2020**, *13*, 4308. [CrossRef] [PubMed]
13. Ali, F.; Ishfaq, N.; Said, A.; Nawaz, Z.; Ali, Z.; Ali, N.; Afzal, A.; Bilal, M. Fabrication, characterization, morphological and thermal investigations of functionalized multi-walled carbon nanotubes reinforced epoxy nanocomposites. *Prog. Org. Coat.* **2021**, *150*, 105962. [CrossRef]
14. Nayak, S.R.; Mohana, K.N.S.; Hegde, M.B.; Rajitha, K.; Madhusudhana, A.M.; Naik, S.R. Functionalized multi-walled carbon nanotube/polyindole incorporated epoxy: An effective anti-corrosion coating material for mild steel. *J. Alloys Compd.* **2021**, *856*, 158057. [CrossRef]
15. Fan, B.; He, D.; Liu, Y.; Bai, J. Influence of Thermal Treatments on the Evolution of Conductive Paths in Carbon Nanotube-Al2O3 Hybrid Reinforced Epoxy Composites. *Langmuir* **2017**, *33*, 9680–9686. [CrossRef] [PubMed]
16. Li, W.; Dichiara, A.; Zha, J.; Su, Z.; Bai, J. On improvement of mechanical and thermo-mechanical properties of glass fabric/epoxy composites by incorporating CNT–Al2O3 hybrids. *Compos. Sci. Technol.* **2014**, *103*, 36–43. [CrossRef]
17. Kocaman, S.; Gursoy, M.; Karaman, M.; Ahmetli, G. Synthesis and plasma surface functionalization of carbon nanotubes for using in advanced epoxy-based nanocomposites. *Surf. Coat. Technol.* **2020**, *399*, 126144. [CrossRef]
18. Mishra, K.; Singh, R.P. Effect of APTMS modification on multiwall carbon nanotube reinforced epoxy nanocomposites. *Compos. Part B Eng.* **2019**, *162*, 425–432. [CrossRef]
19. Marriam, I.; Xu, F.; Tebyetekerwa, M.; Gao, Y.; Liu, W.; Liu, X.; Qiu, Y. Synergistic effect of CNT films impregnated with CNT modified epoxy solution towards boosted interfacial bonding and functional properties of the composites. *Compos. Part A Appl. Sci. Manuf.* **2018**, *110*, 1–10. [CrossRef]
20. Jian, W.; Lau, D. Understanding the effect of functionalization in CNT-epoxy nanocomposite from molecular level. *Compos. Sci. Technol.* **2020**, *191*, 108076. [CrossRef]
21. Khare, K.S.; Khabaz, F.; Khare, R. Effect of Carbon Nanotube Functionalization on Mechanical and Thermal Properties of Cross-Linked Epoxy–Carbon Nanotube Nanocomposites: Role of Strengthening the Interfacial Interactions. *ACS Appl. Mater. Interfaces* **2014**, *6*, 6098–6110. [CrossRef]
22. Ni, Y.; Han, H.; Volz, S.; Dumitrică, T. Nanoscale Azide Polymer Functionalization: A Robust Solution for Suppressing the Carbon Nanotube–Polymer Matrix Thermal Interface Resistance. *J. Phys. Chem. C* **2015**, *119*, 12193–12198. [CrossRef]
23. Saravanan, D.; Palanisamy, C.; Raajeshkrishna, C.R. Tribological performance of multi walled carbon nanotubes–alumina hybrid/epoxy nanocomposites under dry sliding condition. *Mater. Res. Express* **2019**, *6*, 105067. [CrossRef]
24. Li, W.; He, D.; Dang, Z.; Bai, J. In situ damage sensing in the glass fabric reinforced epoxy composites containing CNT–Al2O3 hybrids. *Compos. Sci. Technol.* **2014**, *99*, 8–14. [CrossRef]
25. He, C.N.; Tian, F. A carbon nanotube–alumina network structure for fabricating epoxy composites. *Scr. Mater.* **2009**, *61*, 285–288. [CrossRef]

26. Barral, L.; Díez, F.J.; García-Garabal, S.; López, J.; Montero, B.; Montes, R.; Ramírez, C.; Rico, M. Thermodegradation kinetics of a hybrid inorganic–organic epoxy system. *Eur. Polym. J.* **2005**, *41*, 1662–1666. [CrossRef]
27. Chang, W.L. Decomposition behavior of polyurethanes via mathematical simulation. *J. Appl. Polym. Sci.* **1994**, *53*, 1759–1769. [CrossRef]
28. Liaw, D.J.; Shen, W.C. Curing of acrylated epoxy resin based on bisphenol-S. *Polym. Eng. Sci.* **1994**, *34*, 1297–1303. [CrossRef]
29. Ochi, M.; Tsuyuno, N.; Sakaga, K.; Nakanishi, Y.; Murata, Y. Effect of network structure on thermal and mechanical properties of biphenol-type epoxy resins cured with phenols. *J. Appl. Polym. Sci.* **1995**, *56*, 1161–1167. [CrossRef]
30. Jin, F.-L.; Park, S.-J. Thermal properties of epoxy resin/filler hybrid composites. *Polym. Degrad. Stab.* **2012**, *97*, 2148–2153. [CrossRef]
31. Zhou, Y.; Pervin, F.; Lewis, L.; Jeelani, S. Experimental study on the thermal and mechanical properties of multi-walled carbon nanotube-reinforced epoxy. *Mater. Sci. Eng. A* **2007**, *452*, 657–664. [CrossRef]
32. Yu, A.; Ramesh, P.; Sun, X.; Bekyarova, E.; Itkis, M.E.; Haddon, R.C. Enhanced thermal conductivity in a hybrid graphite nanoplatelet–carbon nanotube filler for epoxy composites. *Adv. Mater.* **2008**, *20*, 4740–4744. [CrossRef]
33. Yang, S.-Y.; Lin, W.-N.; Huang, Y.-L.; Tien, H.-W.; Wang, J.-Y.; Ma, C.-C.M.; Li, S.-M.; Wang, Y.-S. Synergetic effects of graphene platelets and carbon nanotubes on the mechanical and thermal properties of epoxy composites. *Carbon* **2011**, *49*, 793–803. [CrossRef]
34. Kudus, M.H.A.; Akil, H.M.; Mohamad, H.; Loon, L.E. Effect of catalyst calcination temperature on the synthesis of MWCNT–alumina hybrid compound using methane decomposition method. *J. Alloys Compd.* **2011**, *509*, 2784–2788. [CrossRef]
35. Wang, Z.; Qi, R.; Wang, J.; Qi, S. Thermal conductivity improvement of epoxy composite filled with expanded graphite. *Ceram. Int.* **2015**, *41 Pt A*, 13541–13546. [CrossRef]
36. Vasconcelos, G.D.C.; Mazur, R.L.; Ribeiro, B.; Botelho, E.C.; Costa, M.L. Evaluation of decomposition kinetics of poly (ether-ether-ketone) by thermogravimetric analysis. *Mater. Res.* **2014**, *17*, 227–235. [CrossRef]
37. Neĭman, M.; Kovarskaya, B.; Golubenkova, L.; Strizhkova, A.; Levantovskaya, I.; Akutin, M. The thermal degradation of some epoxy resins. *J. Polym. Sci.* **1962**, *56*, 383–389. [CrossRef]
38. Grassie, N.; Guy, M.I.; Tennent, N.H. Degradation of epoxy polymers: Part 4—Thermal degradation of bisphenol-A diglycidyl ether cured with ethylene diamine. *Polym. Degrad. Stab.* **1986**, *14*, 125–137. [CrossRef]
39. Grassie, N.; Guy, M.I.; Tennent, N.H. Degradation of epoxy polymers: Part 1—Products of thermal degradation of bisphenol-A diglycidyl ether. *Polym. Degrad. Stab.* **1985**, *12*, 65–91. [CrossRef]
40. Wang, H.; Tao, X.; Newton, E. Thermal degradation kinetics and lifetime prediction of a luminescent conducting polymer. *Polym. Int.* **2004**, *53*, 20–26. [CrossRef]
41. Xie, W.; Heltsley, R.; Cai, X.; Deng, F.; Liu, J.; Lee, C.; Pan, W.P. Study of stability of high-temperature polyimides using TG/MS technique. *J. Appl. Polym. Sci.* **2002**, *83*, 1219–1227. [CrossRef]
42. Barton, J.; Lee, W.; Wright, W. Some applications of thermal methods of analysis to polymers. *J. Therm. Anal.* **1978**, *13*, 85–98. [CrossRef]